HHS Public Access

Author manuscript

Mol Neurobiol. Author manuscript; available in PMC 2018 May 01.

Published in final edited form as:

Mol Neurobiol. 2017 May ; 54(4): 2659–2673. doi:10.1007/s12035-016-9851-0.

Exosomes derived from mesenchymal stromal cells promote axonal growth of cortical neurons

Yi Zhang[1)], **Michael Chopp**[1),2)], **Xian Shuang Liu**[1)], **Mark Katakowski**[1)], **Xinli Wang**[1)], **Xinchu Tian**[3)], **David Wu**[3)], and **Zheng Gang Zhang**[1),*]

[1)]Department of Neurology, Henry Ford Hospital, Detroit, Michigan, 48202

[2)]Department of Physics, Oakland University, Rochester, Michigan, 48309

[3)]Troy High School, Troy, Michigan, 48098

Abstract

Treatment of brain injury with exosomes derived from mesenchymal stromal cells (MSCs) enhances neurite growth. However, the direct effect of exosomes on axonal growth and molecular mechanisms underlying exosome-enhanced neurite growth are not known. Using primary cortical neurons cultured in a microfluidic device, we found that MSC-exosomes promoted axonal growth, whereas attenuation of argonaut 2 protein, one of the primary microRNA (miRNA) machinery proteins, in MSC-exosomes abolished their effect on axonal growth. Both neuronal cell bodies and axons internalized MSC-exosomes, which was blocked by botulinum neurotoxins (BoNTs) that cleave proteins of the soluble N-ethylmaleimide sensitive factor attachment protein receptor (SNARE) complex. Moreover, tailored MSC-exosomes carrying elevated miR-17-92 cluster further enhanced axonal growth compared to native MSC-exosomes. Quantitative RT-PCR and Western blot analysis showed that the tailored MSC-exosomes increased levels of individual members of this cluster and activated the PTEN/mTOR signaling pathway in recipient neurons, respectively. Together, our data demonstrate that native MSC-exosomes promote axonal growth while the tailored MSC-exosomes can further boost this effect and that tailored exosomes can deliver their selective cargo miRNAs into and activate their target signals in recipient neurons. Neuronal internalization of MSC-exosomes is mediated by the SNARE complex. This study reveals molecular mechanisms that contribute to MSC-exosome-promoted axonal growth, which provides a potential therapeutic strategy to enhance axonal growth.

Keywords

Exosomes; Mesenchymal Stromal Cells; Axon; microRNA

Introduction

Axonal remodeling is a key repair process, leading to reduction of neurological deficits after stroke and traumatic brain injury (TBI). However, spontaneous axonal regeneration is

*To whom correspondence should be addressed: Dr. Zheng Gang Zhang, Department of Neurology, Henry Ford Hospital, 2799 West Grand Boulevard, Detroit, MI 48202. zhazh@neuro.hfh.edu, Tel: 313-916-5456, Fax: 313-916-1318.

limited in adult injured brain [1–3]. There are two major conditions that limit neurite regrowth after brain injury, a diminished intrinsic capacity of the neurons to grow and an inhibitory extrinsic environment [4–7]. However, several lines of evidence indicate that axons can sprout after injury in adult central nervous system [8–12]. Recent studies show that distal axons of embryonic cortical neurons contain miRNA machinery proteins, Dicer and argonaut 2 protein (Ago2) and are enriched with miRNAs that can locally regulate axonal growth [13–15]. For example, alteration of the miR-17-92 cluster and miR-29c levels in the cultured neurons promote axonal growth by suppressing their target genes that inhibit axonal growth even under the inhibitory environment with chondroitin sulfate proteoglycans [16,17].

Exosomes are endosome-derived small membrane vesicles (~30–100 nm) and are released by cells in all living systems [18,19]. Exosomes mediate intercellular communication by transferring proteins, lipids, and genomic materials including mRNAs and miRNAs between source and target cells [20]. Emerging data indicate that treatment of stroke and TBI with exosomes derived from MSCs improves neurological function by facilitating interwoven brain repair processes including neurite remodeling [21–23]. In vitro studies indicate that miR-133b in MSC-exosomes mediate neurite growth of cortical neurons [24]. However, mechanisms underlying the effect of MSC-exosomes on axonal growth remain unknown. Using embryonic cortical neurons cultured in a microfluidic device, we investigated whether MSC-exosomes deliver their cargo miRNAs into recipient neurons and promote axonal growth. Our data demonstrated that miRNAs within MSC-exosomes mediated axonal growth and that tailored MSC-exosomes carrying elevated miR-17-92 cluster enhanced axonal growth to a much greater extent than native MSC-exosomes.

Material and Methods

All experimental procedures were carried out in accordance with the NIH Guide for the Care and Use of Laboratory Animals and approved by the Institutional Animal Care and Use Committee of Henry Ford Hospital.

Neuronal culture in a microfluidic device

Cortical neurons were harvested from embryonic day-18 Wistar rats (Charles River Laboratories, Wilmington, MA) according to the published protocol [25]. Cultures were prepared according to published studies with some modifications [26,16]. Briefly, the isolated cortical neurons were pre-purified by density gradient separation to remove astrocytes, oligodendrocytes and microglia [27] with the purity of more than 95% as reported [28]. The cortical neurons were then seeded in a microfluidic culture device (Standard Neuron Device, Cat# SND450, Xona Microfluidics, Temecula, CA) at density at 3×10^7cells/ml (~3×10^5 cells in the somal compartment). The microfluidic culture device permits distal axons to grow into the axonal compartment after passing 450μm long microgrooves that connect the cell body and axonal compartments [26]. The application of exosomes was performed on Days in Vitro 3 (DIV3), when all of the microgrooves were fully filed with axons. Distal axonal length was imaged in the axonal compartment 24 and

48 hours after exosomal application and at least 15 longest axons per device were analyzed according to our published protocol [17,16].

Time-lapse microscopy to track axonal growth

Primary cortical neurons cultured in a microfluidic device were incubated on a stage top chamber with 5% CO2 at 37°C (Live- Cell Control Unit), which was placed on the stage of a TE2000-U inverted microscope equipped with a motorized z-stage (Nikon, Tokyo, Japan). To track axonal growth, a 20x objective with 1.5x zoom was used for acquiring images in the axonal compartment. A stack of images (10 images of 1 μm steps of the z-axis) was acquired under a bright-field view at 5 min intervals for a total of 60 min using a CCD camera (CoolSnap, 5000) controlled by a Metamoph software (Universal Imaging, West Chester, PA) [29]. Four to 5 individual distal axons with healthy growth cones were imaged and approximately 40 growth cones per experimental group were recorded.

Isolation of MSC-exosomes

Rat primary MSCs were harvested and cultured from the bone marrow of adult Wistar rats (Charles River Laboratories, Wilmington, MA) [24]. Passage 1 MSCs were employed to generate exosomes [24,21]. Briefly, the supernatant of MSCs cultured in exosome depleted growth medium was collected and filtered through a 0.22μm filter (Millipore, CA) to sieve out dead cell and large growth debris. To remove additional debris, the filtered supernatant was run at a 10,000×g for 30 minutes. Ultracentrifugation was then performed at a 100,000×g for 3 hours to collect the exosomes. After that, the supernatant was collected and used for a negative control, whereas the pellet was diluted by sterilized PBS for further characterization and for use of experiments. Numbers and sizes of particles in the pellet were measured and analyzed by means of the qNano® system (IZON, UK).

MSC-exosome labeling

To track internalization of MSC-exosomes, the fresh harvested exosomes were transfected with Texas-red labeled siRNA by means of an exo-fect exosome transfection kit (System Bioscience). Briefly, 3×10^{11} exosomes were incubated with tranfection solution and siRNA at 37°C in a shaker for 10 minutes and then exosome samples were placed on ice for 30 minutes to stop the reaction. Transfected exosomes were collected by 13,000 rpm centrifugation for 30min and re-suspended by 100 μl PBS. These exosomes were immediately applied to the neurons cultured in a microfluidic device.

Generation of tailored MSC exosomes

The majority of miRNAs in exosomes are bounded to Ago2 [30,31]. To examine whether Ago2 is required for the effect of exosomes on axonal growth, we generated MSC-exosomes with reduced Ago2. Briefly, MSCs were transfected with siRNA against Ago2 (GE Dharmacon, siGENOME Ago2 siRNA, M-094504-01) or scramble control (GE Dharmacon, siGENOME Non-Targeting Control siRNAs, D-001210-01) by means of electroporation [16]. Exosomes were isolated from the supernatant of these transfected MSCs cultured in exosome depleted medium as aforementioned. Western blot analysis was performed to measure Ago2 levels in MSCs and MSC-exosomes. To generate tailored MSC-exosomes

carrying elevated miR-17-92 cluster, MSCs were transfected with a miR-17-92 cluster plasmid (pCAG-GFP-miR-17-92) or an empty vector according to our published protocol [16]. Exosomes were harvested from MSCs 72h after transfection. Quantitative RT-PCR was performed to measure individual members of the cluster in exosomes.

Experimental groups

To examine the role of MSC-exosomes on axonal growth, we placed 3×10^9 MSC-exosome into the somal compartment (diluted in 300μl of growth medium) of the microfluidic culture device. In order to test the function of MSC-exosomes to locally promote axonal growth, we applied 3×10^8 (diluted in 300μl of growth medium) MSC-exosomes into the axonal compartment. An equal amount of PBS employed for the dilution of exosomes was used as a control group.

To examine whether the SNARE complex is involved in MSC-exosome internalization by neurons, we employed two BoNTs, α-Bungarotoxin (BoNT/A, Sigma-Aldrich, T0195) for the cleavage of Synaptosomal-Associated Protein 25 (SNAP25) and β-Bungarotoxin (BoNT/B, Santa Cruz, 12778-32-4) for cleavage of vesicle associated membrane protein 2 (VAMP2) [32,33]. Briefly, for the cleavage of neuronal SNAP25, BoNT/A at 100 and 500nM was applied to axonal and somal compartments, respectively, on DIV2, prior to the exosome treatment. For the cleavage of VAMP2 in exosomes, BoNT/B (200nM) was applied to MSC-exosomes for 4 hours. Then these exosomes were placed into the axonal or soma compartment.

To examine the effect of MSC-exosomes on axons under Chondroitin sulfate proteoglycan (CSPG) conditions, 2μg/ml CSPGs (EMD Millipore, CC117) were applied into the axonal compartment of the microfluidic device on DIV2. Twenty-four hours later, the MSC-exosomes were added into either the somal compartment or axonal compartment, respectively, in the presence of CSPGs.

Endocytosis assay

On DIV3, FM 1-43 FX (10μM, F-35355, Life technology) were added into the axonal compartment where axons had been treated with BoNT/A on DIV2 or without the BoNT/A treatment. Twenty minutes later, axons and their parent neuronal somata were then fixed with 4% PFA for 10min, washed with PBS three times. FM 1-43 FX signals in axonal compartments were imaged at 633 nm wavelength by means of confocal microscope (Zeiss LSM 510 NLO, Carl Zeiss, Germany) according to published protocol [34].

Immunocytochemistry

Immunofluorescent staining was performed as previously described [35,17,23] Briefly, after washing with PBS twice and fixation with 4% formaldehyde, axons and neurons in the microfluidic devices were incubated with the primary antibodies for one or two nights at 4°C, and then with Cy3 or FITC conjugated secondary antibodies for 2 hours at room temperature. Nuclei were counterstained with 4′,6-diamidino-2-phenylindole (DAPI, 1:10,000, Vector Laboratories, Burlingame, CA). The following primary antibodies were used: a monoclonal antibody against phosphorylated neurofilament heavy chain (pNFH,

SMI31, 1:500 Covance); a monoclonal antibody against Microtubule-associated protein 2 (MAP2, MAB3418, 1:500 Chemicon),

Image acquisition and quantification

For measurements of axonal elongation after exosome treatment, the distal axons in the axonal compartment were imaged under a 10x objective of an IX71 microscope (OLYMPUS, Tokyo, Japan) using a CCD camera (CoolSnap, 5000) and MetaView software (Universal Imaging, West Chester, PA). Five images per compartment were acquired, which encompassed the majority of the compartment. The lengths of the 15 longest axons in each compartment were measured by tracing individual axons with imageJ according to the published procedures and data are presented as the average length of axons (Mean±SEM, μm) [36].

For analysis of time-lapse images, extension of growth cones (n=~40) was acquired from 6 individual chambers of each experimental group and the extension of growth cones during the experimental period was measured and calculated with Metamorph software (Universal Imaging, West Chester, PA) and data are presented as extension length (Mean±SEM, μm).

For detection of labeled MSC-exosomes and FM 1-43 FX signals in cortical neurons, the cell bodies and axons of the cortical neurons were imaged under a 63x objective after the immunocytochemistry staining using a laser-scanning confocal microscope (Zeiss LSM 510 NLO, Carl Zeiss, Germany) with three laser sources of 488, 543 and 633 nm [29,16]. The images were captured and processed by Laser Scanning Microscope LSM510 (Carl Zeiss, Germany, version 4.2 SP1).

Isolation of proteins and RNAs from axons

The axonal proteins or RNAs were harvested according to published studies [17,16]. Briefly, the growth medium in the axonal compartment was collected, whereas the medium in soma compartment was retained to avoid the backflow of lysis buffer to the soma compartment. The axonal compartment was rinsed 2 times with PBS and then 10 μl of lysis buffer (RIPA for protein harvesting and Qiazol for RNAs, respectively) was added into the axonal compartment for 10 min on ice. The lysate was then collected and reused for an additional microfluidic device in order to concentrate the axonal proteins [17]. For extraction of total RNAs in the axonal compartment, Qiazol lysis buffer was used.

Western blot analysis

Protein concentration of the lysate of the cell body and axonal extracts was determined using a bicinchoninic acid (BCA) protein assay kit (Pierce Biotechnology, Rockford, IL). Western blots were performed according to published methods [16]. Briefly, equal amounts of total protein for each sample were loaded on 10% SDS-polyacrylamide gels. After electrophoresis, the protein was transferred to PVDF membranes, and the blots were subsequently probed with the following primary antibodies: rabbit polyclonal anti-SNAP-25 (1:500; ab5666, Abcam, corresponding to SNAP-25 AA 195-206, which is cleaved out by BoNT/A.), mouse momoclonal anti- VAMP2 (1:500; ab90433, corresponding to VAMP2 AA 33-96), rabbit polyclonal anti- Phosphatase and tensin homolog (PTEN, 1:1000; Cell

Signaling Technology), rabbit polyclonal anti-phosphorylated mechanistic target of rapamycin (mTOR, Ser 2448, 1:1000; Cell Signaling Technology), rabbit polyclonal anti-phosphorylated Glycogen synthase kinase 3β (GSK-3β, Ser 21/9, 1:1000; Cell Signaling Technology), rabbit polyclonal anti-PI3 kinase p85 (1:1000; Millipore), rabbit polyclonal anti-Ras homolog gene family, member A (RhoA, 1:1000; ProteinTech) and mouse monoclonal anti β-actin (1:10000; Abcam, Cambridge, MA). For detection, horseradish peroxidase-conjugated secondary antibodies were used (1:2000) followed by enhanced chemiluminescence development (Pierce Biotechnology). Protein levels of *β*-actin and PI3K subunit p85 were used as the internal controls for somata and axons, respectively [37]. Western blots were performed from at least 3 individual experiments. The optical density of protein signals was quantified using an image processing and analysis program (Scion image, Ederick, MA).

Total proteins from MSC-exosomes were collected using 2X lysis buffer (RIPA, sigma) to lyse exosome samples. The following primary antibodies were used to detect proteins in exosomes: mouse monoclonal anti-Alix (1:500; Cell Signaling), rabbit polyclonal anti-Hsp70 (1:500, Abcam), and rabbit polyclonal anti-VAMP2 (1:500, ab3347, Abcam).

Isolation of total RNA and Real-Time Reverse Transcriptase-Polymerase Chain Reaction

To analyze miRNAs, total RNA was isolated using the miRNeasy Mini kit (Qiagen, Valencia, CA, USA). Quantitative RT-PCR was performed on an ABI 7000 and ABI ViiA™ 7 PCR instrument (Applied Biosystems, Foster City, CA). miRNAs were reversely transcribed with the miRNA Reverse Transcription kit (Applied Biosystems, Foster City, CA, USA) and amplified with the TaqMan miRNA assay (Applied Biosystems), which is specific for mature miRNA sequences. The following specific primers were used: miR-17 (mature sequence: CAAAGUGCUUACAGUGCAGGUAG), miR-18a (mature sequence: UAAGGUGCAUCUAGUGCAGAUAG), miR-19a (mature sequence: UGUGCAAAUCUAUGCAAAACUGA), miR-19b (mature sequence: UGUGCAAAUCCAUGCAAAACUGA), miR-20a (mature sequence: UAAAGUGCUUAUAGUGCAGGUAG), miR-92 (mature sequence: UAUUGCACUUGUCCCGGCCUG), and U6 snRNA (mature sequence: GTGCTCGCTTCGGCAGCACATATACTAAAATTGGAACGATACAGAGAAGATTAGCA TG GCCCCTGCGCAAGGATGACACGCAAATTCGTGAAGCGTTCCATATTTT). Analysis of gene expression was carried out by the $2^{-\Delta\Delta Ct}$ method [38].

Statistical analysis

All statistical analysis was performed using the Statistical Package for the Social Sciences (SPSS, version 11.0; SPSS Inc, Chicago, IL). One-way ANOVA with *post hoc* Bonferroni tests was used when comparing more than two groups. Student's t test was used when comparing two groups. Values presented in this study are expressed as mean ± standard error of the mean (SEM). A p-value < 0.05 was considered to be significant.

Results

Exosomes derived from MSCs promoted axonal growth

To examine the effect of exosomes on axonal growth, we isolated exosomes from cultured MSCs. MSC-exosomes had a mean diameter of 104 nm (Fig. 1) and Western blot analysis showed that these exosomes contained Alix and Hsp70 proteins, markers of exosomes (Fig. 1), which are consistent with MSC-exosome characteristics [24]. We found that exosomes applied to the cell body compartment significantly increased length of the distal axons by 33% and 24% at 24 and 48h in culture, respectively, compared to the distal axons of cortical neurons cultured without exosomes (Fig. 1D, E). To further examine the soma application of exosomes on promoting axonal growth, axonal growth of the cultured neurons treated with or without exosomes for 24 and 48h was monitored in real-time by means of the time-lapse microscopy. During a 60 minute observation period, we detected that the speed of distal axonal elongation was 13±2 μm/h and 13±1μm for neurons treated with exosomes for 24 and 48h, respectively, whereas the axonal elongation in the neurons without treatment with exosomes occured at the speed of 8±1 μm/h and 10 ±1 μm/h for these two time points ($p<0.001$, Fig. 1F, G). Collectively, these data demonstrated that application of MSCs-derived exosomes into cell bodies of cortical neurons promotes distal axon growth.

We then examined whether axonal application of naïve MSC-exosomes locally increases axonal growth. In preliminary experiments, we found that axonal application of the exosomes at a concentration of 3×10^9 particles/ml induced axonal damage including axonal retraction, while concentrations of 3×10^7 and 3×10^8 particles/ml did not cause axonal damage. Thus, a concentration of 3×10^8 particles/ml was employed to axonal application of exosomes in the following experiments. Unlike the soma application of exosomes, the application of exosomes into the axonal compartment for 24h did not significantly increase distal axonal growth (341±14 μm vs 297±9 μm in control group, $p>0.05$, $n=6$). However, the axonal application of exosomes for 48h significantly ($p<0.001$) increased length of distal axons (Fig. 2A). Time-lapse microscopic experiments showed that the axonal application of exosomes for 48h increased the speed of distal axonal elongation by 50% ($p<0.05$), from 10±1 μm/h in the control group to 15±2 μm/h in the exosome group (Fig. 2B–D). These data indicate that in addition to cell bodies, the axonal application of exosomes locally regulates axonal growth.

The SNARE complex is required for neuronal internalization of MSC-exosomes

To examine whether exosomes enter into neurons, we tracked MSC-exosomes transfected with fluorescently labeled siRNA in cultured cortical neurons. The transfected exosomes were added into the cell body or the axonal compartment. The neurons and distal axons were imaged 24h after application of the exosomes by means of a confocal microscope. For the cell body application of labeled exosomes, the fluorescent particles were detected in the cytoplasm of neurons, whereas fluorescent signals were not detected in the axonal compartment (Fig. 3A). For the axonal application, fluorescent particles were only found in the axonal compartment and fluorescent signals were localized along the axons and within the growth cones (Fig. 3B). These data suggest that the cortical neurons internalize MSC-exosomes.

SNARE proteins regulate the synaptic vesicle transcytosis [33,39]. BoNT/B is responsible for synaptobrevin-2, VAMP2, cleavage, whereas BoNT/A cleaves a peripheral plasma membrane protein SNAP25 [40,41]. Western blot analysis of MSC-exosomes and cortical neurons revealed that the exosomes contained VAMP2 proteins, while neurons expressed SNAP-25 (Fig. 4B). To examine whether SNARE proteins are involved in the observed exosome internalization, exosomes were pretreated with BoNT/B and then were applied into the cell body or the axonal compartment. Compared to exosomes without pretreatment, BoNT/B-pretreated exosomes placed in either the cell body or the axonal compartment did not increase axonal growth (Fig. 4A), Moreover, confocal microscopic analysis revealed that BoNT/B-pretreated exosomes identified by fluorescent particles were randomly distributed in the somal or the axonal compartments of the microfluidic culture device and that few of them were detected within the neuronal cytoplasm and axons (Fig. 3C). MSC-exosomes treated with BoNT/B exhibited significant reduction of VAMP2, whereas BoNT/B pretreatment did not affect Alix protein levels in exosomes compared to non-treatment (Fig. 4B), suggesting that BoNT/B specifically acts on VAMP2.

We then examined the effect of BoNT/A on neuronal internalization of MSC-exosomes. Pre-soma application of BoNT/A (500nM) for 24h significantly blocked exosome-increased axonal growth compared to the axonal application of exosomes only (Fig. 4C). Pre-axonal application of BoNT/A (100nM) also abolished the effect of the soma application of exosomes on increased axonal growth (Fig. 4C). The time-lapse microscopic analysis showed that pre-application of BoNT/A either to the soma compartment or the axonal compartment substantially ($p<0.05$) reduced the speed of growth cone extension increased by exosomes (Fig. 4D). Western blot analysis revealed that pre-application of BoNT/A itself either into the soma or the axonal compartment robustly reduced SNAP25 proteins in the somata and axons (Fig. 4E, F). However, BoNT/A itself did not significantly affect axonal growth, but robustly reduced uptake of FM 1–43 FX dye in growth cone (Fig. 4G, H), suggesting that BoNT/A affects endocytosis. Collectively, these data suggest that SNARE proteins participate the process of exosome internalization into axons and cytoplasm of cortical neurons.

To exclude the possibility that exosome-enhanced axonal growth is induced by extra-exosomal cellular RNAs, exosomes were treated with RNase A that digests extra-exosomal cellular RNAs, but preserves RNAs within exosomes [42]. Application of exosomes treated with RNase A (1μg/ml) into the soma or the axonal compartment for 24 or 48h, respectively, significantly increased axonal growth compared to the controls (442±14 vs 297±9 μm in control for the soma and 670±32 vs 505±16 μm in control for the axon, $p<0.05$, n=3/group), which was comparable to applications of the naïve exosomes. We then sonicated exosomes for 10 seconds to destroy exosomes. The effect of exosomes on enhancement of axonal growth was abolished when sonicated exosomes were applied either to the soma or the axonal compartment for 24 (305±23 vs 297±9 μm in control group, $p>0.05$, n=3) or 48h (297±12 vs 297±9 μm in control group, $p>0.05$, n=3), respectively. These data suggest that RNAs and proteins within MSC exosomes play a role in exosome-increased axonal growth.

Ago2 is required for exosome-promoted axonal growth

Ago2 protein, a component of the RNA induced silencing complex (RISC), is the key regulator of miRNA function by mediating the activity of miRNA-guided mRNA cleavage or translational inhibition [43,44]. Exosomes contain Ago2 [45,31,30]. Consistent with published data, our Western blots showed the presence of Ago2 protein in MSC-exosomes (Fig. 5A). We then examined whether Ago2 is involved in the exosome-increased axonal growth by reduction of Ago2 in exosomes. MSCs were transfected with siRNA-Ago2 and exosomes were harvested from supernatant of these MSCs. Western blot analysis revealed that compared to transfection with scramble probes, siRNA-Ago2 transfection substantially reduced Ago2 proteins in MSCs and nearly abolished Ago2 in exosomes (Fig. 5A), indicating that transfection effectively suppresses Ago2 expression. As expected, application of exosomes from the MSCs transfected with scramble siRNA into the soma compartment promoted axonal growth. However, the soma application of Ago2-reduced exosomes did not significantly increase axonal growth (Fig. 5B, C). These data suggest that Ago2 in MSC-exosomes is required for exosome-increased axonal growth.

miRNAs within exosomes are bound to Ago2 [30]. To examine whether reduction of Ago2 levels in exosomes affects miRNA content, miRNA array analysis was performed. Compared to miRNAs within exosomes from MSCs transfected with scramble siRNAs, approximately 76% of miRNAs were reduced in Ago2-reduced exosomes (Table 1), suggesting that exosomes may deliver miRNAs into the axon, mediating exosome-increased axonal growth.

Exosomes with elevated miR-17-92 cluster further promote axonal growth

We then examined the effect of tailored exosomes with elevation of the miR-17-92 cluster on axonal growth based on published studies showing that the miR-17-92 cluster regulates axonal growth [16]. MSCs were transfected with a miR-17-92 cluster plasmid or an empty vector. Exosomes were then harvested from supernatant of these MSCs. Quantitative real-time RT-PCR analysis of the harvested exosomes showed that levels of all individual six members of the miR-17-92 cluster were increased within exosomes isolated from MSCs transfected with the miR-17-92 cluster (miR-17-92-exosomes) compared to levels within exosomes from MSCs transfected with the empty vector (empty-vector-exosomes, Fig. 6A). Application of the empty-vector-exosomes into the soma compartment significantly increased axonal growth, compared to without exosome treatment, which was comparable to naïve exosome-enhanced axonal growth (Fig. 6B, C). These data suggest that transfection itself did not affect exosome-increased axonal growth. However, compared to the empty-vector-exosomes, the miR-17-92-exosomes increased axonal growth by 47% ($p<0.001$, Fig. 6B, C). The time-lapse microscopic analysis showed that the miR-17-92-exosomes increased axonal growth speed (17±2 μm/h, n=43 axons vs 13±1 μm/h, n=44 axons for the empty-vector-exosomes, $p<0.05$) (Fig. 6D). Consistent with soma application of the tailored exosomes, axonal application of the miR17-92-exosomes also significantly increased axonal elongation and axonal growth speed compared to the axonal application of the empty-vector-exosomes (Fig. 6E, F).

To examine whether elevated miR-17-92 cluster in exosomes affects the cluster levels in recipient neurons and axons, levels of individual members of the cluster were measured. Quantitative real-time RT-PCR analysis showed that soma application of the miR17-92-exosomes significantly increased levels of individual members of the cluster in the recipient neurons and axons (Fig. 7A). Furthermore, Western blot analysis showed that levels of PTEN, one of validated targets by the miR-17-92 cluster, were substantially reduced in the neurons and axons treated with the naïve or the empty-vector-exosomes compared to the non-exosome treatment (Fig. 7B, C). Treatment with the miR-17-92-exosomes further decreased the PTEN levels in neurons and axons compared to the empty-vector-exosome treatment (Fig. 7B, C). Reduction of PTEN protein in neurons and axons was associated with elevation of phosphorylated mTOR and GSK-3β proteins, two well known PTEN downstream proteins (Fig. 7B, C). Collectively, these data indicate that exosomes deliver the miR17-92 cluster into recipient neurons and axons and that the miR-17-92 cluster interacts with its target gene PTEN.

Exosomes with elevated miR-17-92 overcome the inhibitory effect of CSPGs

The extracellular matrix inhibitory effect on axonal growth evoked by brain injury is the major obstacle for the regeneration of axons [46–48]. CSPGs expressed by glial cells are inhibitory factors present after injury [49]. We previously found miRNAs in axons modulate the inhibitory effect of CSPGs [23]. Since we demonstrated that the miR-17-92 cluster within tailored enriched miR-17-92 exosomes is delivered into axons, we assessed whether MSC-exosomes overcome the inhibition of CSPGs on axonal growth. We found that 2μg/ml CSPGs applied into the axonal compartment significantly inhibited axonal growth by 36% ($p<0.05$, Fig 8A). As we expected, the application of naïve or empty-vector-exosomes into the soma compartment for 24h reversed the inhibition caused by CSPGs, respectively. Moreover, the miR-17-92-exosomes showed substantially enhanced promotion of axonal growth under CSPG conditions ($p<0.05$, Fig 8A, Soma). Similarly, application of naïve or empty-vector-exosomes into the axonal compartment for 48h also reversed the CSPG inhibitory effect on axonal growth. Addition of the miR-17-92-exosomes into the axonal compartment further enhanced the axonal growth under CSPG conditions by 38% ($p<0.05$, Fig 8A, Axon). The time-lapse microscopic analysis also showed that the miR-17-92-exosomes substantially increased axonal growth speed under CSPG condition either when they were applied into the soma compartment for 24h (13±2 μm/h, n=40 axons vs 4±1 μm/h, n=42 axons for CSPGs treated axons, $p<0.05$) (Fig 8B) or applied into the axonal compartment for 48h (14±2 μm/h, n=35 axons vs 5±1 μm/h, n=41 axons for CSPGs treated axons, $p<0.05$) (Fig. 8C). Together, these data demonstrated that the naïve and tailored MSC-exosomes overcome the CSPG inhibitory effect on axonal growth, whereas tailored exosomes further enhanced the growth.

Discussion

The present study demonstrates that exosomes derived from MSCs promoted axonal growth of cultured cortical neurons. Internalization of MSC-exosomes into neurons and distal axons was mediated by SNARE complex. Reduction of Ago2 in MSC-exosomes abolished exosome-promoted axonal growth. Importantly, tailored MSC-exosomes with elevated

miR-17-92 cluster further enhanced axonal growth via the PTEN/mTOR signals in the neurons, when the exosomes were applied into the soma or axonal compartments even under the CSPG inhibitory environment. These data suggest that MSC-derived exosomes communicate with cortical neurons to enhance axonal growth by transferring biological materials, in particular miRNAs, which provides not only new insights into molecular mechanisms underlying axonal remodeling enhanced by MSC cell therapy, but also proof of principle for exosomes as cargo to deliver specific miRNAs into axons of the cortical neurons.

Cellular and molecular mechanisms underlying MSC therapy to enhance neurological outcomes after brain injury are not fully understood, although it is known that treatment of the injured brain with MSCs stimulates endogenous brain repair processes [50–54]. The present study demonstrated that exosomes derived from MSCs promoted axonal growth of the cortical neurons, suggesting that exosomes released from grafted MSCs could communicate with endogenous neurons in injured brain to enhance axonal growth. Indeed, we recently showed that intravenous administration of MSC-exosomes to animals subjected to stroke or TBI enhanced brain repair and improved neurological function at the levels that are comparable to the MSC therapy [22,23]. Others have shown that exosomes derived from myelinating cells, oligodendrocytes and Schwann cells, communicate with cortical and dorsal root ganglia (DRG) neurons, respectively, to regulate axonal function [55,56].

Exosomes contain biomaterials including proteins, DNAs, RNAs and miRNAs. Using several approaches, the present study demonstrated that miRNAs within MSC-exosomes mediate MSC-exosome enhanced axonal growth. The catalytic activity of Ago2 in miRNA RISC regulates biological function of mature miRNAs by cleaving the target mRNAs [57]. Ablation and overexpression of Ago2 decreases and increases, respectively, the miRNA stability [58]. MiRNAs within exosomes are bound to Ago2 and knockout of Ago2 leads to decrease of miRNA abundance within exosomes[30]. Consistent with those published studies, we found that MSC-exosomes contained Ago2. Reduction of Ago2 protein within the exosomes resulted in decrease of exosomal miRNAs and abolished MSC-exosome promoted axonal growth. In addition, the present study demonstrated that tailored exosomes carrying elevated miR-17-92 cluster can further enhance axonal growth even in the presence of the extracellular CSPG inhibitors compared to naïve MSC-exosomes, which is likely caused by interactions between the miR-17-92 cluster within the exosomes and its target gene, PTEN, within recipient neurons. We have shown that the miR-17-92 cluster within distal axons of cortical neurons locally promotes axonal growth by targeting PTEN/mTOR signals [16]. Others also demonstrate that miR-338[59], miR-132[13], miR-9 [60], miR-8[61] are enriched in distal axons and regulate their target genes involving energy metabolism and cytoskeleton function leading to modulating axonal growth. Distal axons contain miRNA machinery proteins [60,59,16,13]. The PTEN/mTOR signaling pathway has been demonstrated to mediate axonal growth after CNS injury [62,63]. CSPGs block axonal sprouting in ischemic brain [46,64,65]. The present study suggests that activation of intrinsic axon growth signals by tailored exosomes carrying elevated miR-17-92 cluster can overcome an inhibitory extrinsic environment. Thus, tailored exosomes carrying specific miRNAs that mediate axonal growth have enormous therapeutic potential to enhance axonal growth.

The present study showed that compared to the axonal growth increased by the cell body treatment, the axonal application of MSC-exosomes required an additional 24h to augment axonal growth, although the exosomes were internalized by the cell bodies and axons 24h after the cell body and distal axon applications of the exosomes, respectively. The cause of this delay is currently unknown. Other than the local storage of mRNAs in distal axon, mRNAs via RNA binding proteins are transported from the cell body to the axon in response to the extracellular signals [66–68]. We speculate that in addition to interaction with local genes in the distal axon, miRNAs delivered by the exosomes into distal axons may retrogradely communicate with genes in the cell body, leading to transport of proteins from the cell body to the distal axons and thereby increasing axonal growth. Exosomes are membrane vesicles and can be internalized by recipient cells [69,70]. Endocytosis is one of the major routes that mediate exosome internalization by recipient cells [69,71]. Factors that regulate endocytosis including clathrin [71], caveolae [72], lipid raft [73], and macropinocytosis [74], affect exosomal internalization by recipient cells. Protein interactions between exosomes and recipient cells are required for exosomal internalization. For example, when exosomes are treated with proteinase K, the uptake of the exosomes is substantially reduced by ovarian cancer cells [75]. The SNARE complex acts as the regulator for the vesicle exocytosis at the presynaptic compartment, and mediates the docking and fusion of vesicles to membrane compartments, which lead to the release of the neurotransmitter into the synaptic cleft after an action potential [33,76]. Recent studies found that two major components which assemble SNARE complex, synaptobrevin/VAMP at the vesicle membrane and SNAP25 at the plasma membrane, also modulate the vesicle endocytosis at synapses, indicating a dual role of SNARE complex on vesicle transport [77,39]. The present study demonstrated that cleavage of VAMP2 in MSC-exosomes and cleavage of SNAP-25 in cortical neurons blocked of internalization of MSC-exosomes, indicating that the SNARE complex mediates neuronal uptake of MSC-exosomes. Our unpublished data showed that VAMP2 was not present in exosomes isolated from cerebral endothelial cells. Additional studies are warranted to examine whether the SNARE complex regulates neuronal uptake of exosomes is specific to MSC-exosomes.

Acknowledgments

This work was supported by National Institutes of Health (RO1 NS088656 and RO1 NS75156)

References

1. Horner PJ, Gage FH. Regenerating the damaged central nervous system. Nature. 2000; 407(6807): 963–970. DOI: 10.1038/35039559 [PubMed: 11069169]
2. Chen MS, Huber AB, van der Haar ME, Frank M, Schnell L, Spillmann AA, Christ F, Schwab ME. Nogo-A is a myelin-associated neurite outgrowth inhibitor and an antigen for monoclonal antibody IN-1. Nature. 2000; 403(6768):434–439. DOI: 10.1038/35000219 [PubMed: 10667796]
3. Morgenstern DA, Asher RA, Fawcett JW. Chondroitin sulphate proteoglycans in the CNS injury response. Prog Brain Res. 2002; 137:313–332. [PubMed: 12440375]
4. Ueno Y, Chopp M, Zhang L, Buller B, Liu Z, Lehman NL, Liu XS, Zhang Y, Roberts C, Zhang ZG. Axonal outgrowth and dendritic plasticity in the cortical peri-infarct area after experimental stroke. Stroke. 2012; 43(8):2221–2228. STROKEAHA.111.646224 [pii]. DOI: 10.1161/STROKEAHA.111.646224 [PubMed: 22618383]

5. Chaudhry N, Filbin MT. Myelin-associated inhibitory signaling and strategies to overcome inhibition. J Cereb Blood Flow Metab. 2007; 27(6):1096–1107. DOI: 10.1038/sj.jcbfm.9600407 [PubMed: 17033690]
6. Fitch MT, Silver J. CNS injury, glial scars, and inflammation: Inhibitory extracellular matrices and regeneration failure. Exp Neurol. 2008; 209(2):294–301. DOI: 10.1016/j.expneurol.2007.05.014 [PubMed: 17617407]
7. Singh P, Yan J, Hull R, Read S, O'Sullivan J, Henderson RD, Rose S, Greer JM, McCombe PA. Levels of phosphorylated axonal neurofilament subunit H (pNfH) are increased in acute ischemic stroke. J Neurol Sci. 2011; 304(1–2):117–121. DOI: 10.1016/j.jns.2011.01.025 [PubMed: 21349546]
8. Snyder EY, Yoon C, Flax JD, Macklis JD. Multipotent neural precursors can differentiate toward replacement of neurons undergoing targeted apoptotic degeneration in adult mouse neocortex. Proc Natl Acad Sci U S A. 1997; 94(21):11663–11668. [PubMed: 9326667]
9. Brustle O, Jones KN, Learish RD, Karram K, Choudhary K, Wiestler OD, Duncan ID, McKay RD. Embryonic stem cell-derived glial precursors: a source of myelinating transplants. Science. 1999; 285(5428):754–756. [PubMed: 10427001]
10. Stichel CC, Muller HW. Experimental strategies to promote axonal regeneration after traumatic central nervous system injury. Prog Neurobiol. 1998; 56(2):119–148. [PubMed: 9760698]
11. Ayaz D, Leyssen M, Koch M, Yan J, Srahna M, Sheeba V, Fogle KJ, Holmes TC, Hassan BA. Axonal injury and regeneration in the adult brain of Drosophila. J Neurosci. 2008; 28(23):6010–6021. DOI: 10.1523/JNEUROSCI.0101-08.2008 [PubMed: 18524906]
12. Liu Z, Chopp M, Ding X, Cui Y, Li Y. Axonal remodeling of the corticospinal tract in the spinal cord contributes to voluntary motor recovery after stroke in adult mice. Stroke. 2013; 44(7):1951–1956. DOI: 10.1161/STROKEAHA.113.001162 [PubMed: 23696550]
13. Hancock ML, Preitner N, Quan J, Flanagan JG. MicroRNA-132 is enriched in developing axons, locally regulates Rasa1 mRNA, and promotes axon extension. J Neurosci. 2014; 34(1):66–78. 34/1/66 [pii]. DOI: 10.1523/JNEUROSCI.3371-13.2014 [PubMed: 24381269]
14. Sasaki Y, Gross C, Xing L, Goshima Y, Bassell GJ. Identification of axon-enriched microRNAs localized to growth cones of cortical neurons. Dev Neurobiol. 2014; 74(3):397–406. DOI: 10.1002/dneu.22113 [PubMed: 23897634]
15. Kim HH, Kim P, Phay M, Yoo S. Identification of precursor microRNAs within distal axons of sensory neuron. J Neurochem. 2015; 134(2):193–199. DOI: 10.1111/jnc.13140 [PubMed: 25919946]
16. Zhang Y, Ueno Y, Liu XS, Buller B, Wang X, Chopp M, Zhang ZG. The MicroRNA-17-92 cluster enhances axonal outgrowth in embryonic cortical neurons. J Neurosci. 2013; 33(16):6885–6894. 33/16/6885 [pii]. DOI: 10.1523/JNEUROSCI.5180-12.2013 [PubMed: 23595747]
17. Zhang Y, Chopp M, Liu X, Kassis H, Wang X, Li C, An G, Gang Zhang Z. MicroRNAs in the axon locally mediate the effects of chondroitin sulfate proteoglycans and cGMP on axonal growth. Dev Neurobiol. 2015; doi: 10.1002/dneu.22292
18. Fevrier B, Raposo G. Exosomes: endosomal-derived vesicles shipping extracellular messages. Curr Opin Cell Biol. 2004; 16(4):415–421. DOI: 10.1016/j.ceb.2004.06.003 [PubMed: 15261674]
19. Raposo G, Stoorvogel W. Extracellular vesicles: exosomes, microvesicles, and friends. J Cell Biol. 2013; 200(4):373–383. DOI: 10.1083/jcb.201211138 [PubMed: 23420871]
20. Braicu C, Tomuleasa C, Monroig P, Cucuianu A, Berindan-Neagoe I, Calin GA. Exosomes as divine messengers: are they the Hermes of modern molecular oncology? Cell Death Differ. 2015; 22(1):34–45. DOI: 10.1038/cdd.2014.130 [PubMed: 25236394]
21. Xin H, Li Y, Liu Z, Wang X, Shang X, Cui Y, Zhang ZG, Chopp M. MiR-133b promotes neural plasticity and functional recovery after treatment of stroke with multipotent mesenchymal stromal cells in rats via transfer of exosome-enriched extracellular particles. Stem Cells. 2013; 31(12):2737–2746. DOI: 10.1002/stem.1409 [PubMed: 23630198]
22. Xin H, Li Y, Cui Y, Yang JJ, Zhang ZG, Chopp M. Systemic administration of exosomes released from mesenchymal stromal cells promote functional recovery and neurovascular plasticity after stroke in rats. J Cereb Blood Flow Metab. 2013; 33(11):1711–1715. jcbfm2013152 [pii]. DOI: 10.1038/jcbfm.2013.152 [PubMed: 23963371]

23. Zhang Y, Chopp M, Meng Y, Katakowski M, Xin H, Mahmood A, Xiong Y. Effect of exosomes derived from multipluripotent mesenchymal stromal cells on functional recovery and neurovascular plasticity in rats after traumatic brain injury. Journal of neurosurgery. 2015; 122(4): 856–867. DOI: 10.3171/2014.11.JNS14770 [PubMed: 25594326]
24. Xin H, Li Y, Buller B, Katakowski M, Zhang Y, Wang X, Shang X, Zhang ZG, Chopp M. Exosome-mediated transfer of miR-133b from multipotent mesenchymal stromal cells to neural cells contributes to neurite outgrowth. Stem Cells. 2012; 30(7):1556–1564. DOI: 10.1002/stem.1129 [PubMed: 22605481]
25. Taylor AM, Rhee SW, Tu CH, Cribbs DH, Cotman CW, Jeon NL. Microfluidic Multicompartment Device for Neuroscience Research. Langmuir. 2003; 19(5):1551–1556. DOI: 10.1021/la026417v [PubMed: 20725530]
26. Taylor AM, Blurton-Jones M, Rhee SW, Cribbs DH, Cotman CW, Jeon NL. A microfluidic culture platform for CNS axonal injury, regeneration and transport. Nature methods. 2005; 2(8):599. [PubMed: 16094385]
27. Brewer GJ, Torricelli JR. Isolation and culture of adult neurons and neurospheres. Nat Protoc. 2007; 2(6):1490–1498. nprot.2007.207 [pii]. DOI: 10.1038/nprot.2007.207 [PubMed: 17545985]
28. Xu SY, Wu YM, Ji Z, Gao XY, Pan SY. A modified technique for culturing primary fetal rat cortical neurons. Journal of biomedicine & biotechnology. 2012; 2012:803930.doi: 10.1155/2012/803930 [PubMed: 23193366]
29. Zhang RL, Chopp M, Gregg SR, Toh Y, Roberts C, Letourneau Y, Buller B, Jia L, SPND, Zhang ZG. Patterns and dynamics of subventricular zone neuroblast migration in the ischemic striatum of the adult mouse. J Cereb Blood Flow Metab. 2009; 29(7):1240–1250. jcbfm200955 [pii]. DOI: 10.1038/jcbfm.2009.55 [PubMed: 19436318]
30. Guduric-Fuchs J, O'Connor A, Camp B, O'Neill CL, Medina RJ, Simpson DA. Selective extracellular vesicle-mediated export of an overlapping set of microRNAs from multiple cell types. BMC Genomics. 2012; 13:357.doi: 10.1186/1471-2164-13-357 [PubMed: 22849433]
31. Melo SA, Sugimoto H, O'Connell JT, Kato N, Villanueva A, Vidal A, Qiu L, Vitkin E, Perelman LT, Melo CA, Lucci A, Ivan C, Calin GA, Kalluri R. Cancer exosomes perform cell-independent microRNA biogenesis and promote tumorigenesis. Cancer Cell. 2014; 26(5):707–721. DOI: 10.1016/j.ccell.2014.09.005 [PubMed: 25446899]
32. Pecho-Vrieseling E, Rieker C, Fuchs S, Bleckmann D, Esposito MS, Botta P, Goldstein C, Bernhard M, Galimberti I, Muller M, Luthi A, Arber S, Bouwmeester T, van der Putten H, Di Giorgio FP. Transneuronal propagation of mutant huntingtin contributes to non-cell autonomous pathology in neurons. Nat Neurosci. 2014; 17(8):1064–1072. nn.3761 [pii]. DOI: 10.1038/nn.3761 [PubMed: 25017010]
33. Sudhof TC, Rizo J. Synaptic vesicle exocytosis. Cold Spring Harb Perspect Biol. 2011; 3(12) a005637 [pii] cshperspect.a005637 [pii]. doi: 10.1101/cshperspect.a005637
34. Gracias NG, Shirkey-Son NJ, Hengst U. Local translation of TC10 is required for membrane expansion during axon outgrowth. Nat Commun. 2014; 5:3506.doi: 10.1038/ncomms4506 [PubMed: 24667291]
35. Liu XS, Chopp M, Zhang RL, Hozeska-Solgot A, Gregg SC, Buller B, Lu M, Zhang ZG. Angiopoietin 2 mediates the differentiation and migration of neural progenitor cells in the subventricular zone after stroke. J Biol Chem. 2009; 284(34):22680–22689. M109.006551 [pii]. DOI: 10.1074/jbc.M109.006551 [PubMed: 19553662]
36. Meijering E, Jacob M, Sarria JC, Steiner P, Hirling H, Unser M. Design and validation of a tool for neurite tracing and analysis in fluorescence microscopy images. Cytometry A. 2004; 58(2):167–176. DOI: 10.1002/cyto.a.20022 [PubMed: 15057970]
37. Andreassi C, Zimmermann C, Mitter R, Fusco S, Devita S, Saiardi A, Riccio A. An NGF-responsive element targets myo-inositol monophosphatase-1 mRNA to sympathetic neuron axons. Nature Neuroscience. 2010; 13(3):291–301. DOI: 10.1038/nn.2486 [PubMed: 20118926]
38. Livak KJ, Schmittgen TD. Analysis of relative gene expression data using real-time quantitative PCR and the 2(−Delta Delta C(T)) Method. Methods. 2001; 25(4):402–408. DOI: 10.1006/meth.2001.1262 [PubMed: 11846609]

39. Zhang Z, Wang D, Sun T, Xu J, Chiang HC, Shin W, Wu LG. The SNARE proteins SNAP25 and synaptobrevin are involved in endocytosis at hippocampal synapses. J Neurosci. 2013; 33(21): 9169–9175. DOI: 10.1523/JNEUROSCI.0301-13.2013 [PubMed: 23699527]
40. Chen S, Hall C, Barbieri JT. Substrate recognition of VAMP-2 by botulinum neurotoxin B and tetanus neurotoxin. J Biol Chem. 2008; 283(30):21153–21159. DOI: 10.1074/jbc.M800611200 [PubMed: 18511417]
41. Peng L, Liu H, Ruan H, Tepp WH, Stoothoff WH, Brown RH, Johnson EA, Yao WD, Zhang SC, Dong M. Cytotoxicity of botulinum neurotoxins reveals a direct role of syntaxin 1 and SNAP-25 in neuron survival. Nat Commun. 2013; 4:1472.doi: 10.1038/ncomms2462 [PubMed: 23403573]
42. Koga Y, Yasunaga M, Moriya Y, Akasu T, Fujita S, Yamamoto S, Matsumura Y. Exosome can prevent RNase from degrading microRNA in feces. J Gastrointest Oncol. 2011; 2(4):215–222. DOI: 10.3978/j.issn.2078-6891.2011.015 [PubMed: 22811855]
43. Macfarlane LA, Murphy PR. MicroRNA: Biogenesis, Function and Role in Cancer. Curr Genomics. 2010; 11(7):537–561. DOI: 10.2174/138920210793175895 [PubMed: 21532838]
44. Meister G. Argonaute proteins: functional insights and emerging roles. Nature reviews Genetics. 2013; 14(7):447–459. DOI: 10.1038/nrg3462
45. Gibbings DJ, Ciaudo C, Erhardt M, Voinnet O. Multivesicular bodies associate with components of miRNA effector complexes and modulate miRNA activity. Nat Cell Biol. 2009; 11(9):1143–1149. DOI: 10.1038/ncb1929 [PubMed: 19684575]
46. Yiu G, He Z. Glial inhibition of CNS axon regeneration. Nat Rev Neurosci. 2006; 7(8):617–627. DOI: 10.1038/nrn1956 [PubMed: 16858390]
47. Toy D, Namgung U. Role of glial cells in axonal regeneration. Experimental neurobiology. 2013; 22(2):68–76. DOI: 10.5607/en.2013.22.2.68 [PubMed: 23833555]
48. Filbin MT. Myelin-associated inhibitors of axonal regeneration in the adult mammalian CNS. Nat Rev Neurosci. 2003; 4(9):703–713. DOI: 10.1038/nrn1195 [PubMed: 12951563]
49. Haas CA, Rauch U, Thon N, Merten T, Deller T. Entorhinal cortex lesion in adult rats induces the expression of the neuronal chondroitin sulfate proteoglycan neurocan in reactive astrocytes. J Neurosci. 1999; 19(22):9953–9963. [PubMed: 10559403]
50. Xiong Y, Mahmood A, Chopp M. Angiogenesis, neurogenesis and brain recovery of function following injury. Curr Opin Investig Drugs. 2010; 11(3):298–308.
51. Zhang ZG, Chopp M. Neurorestorative therapies for stroke: underlying mechanisms and translation to the clinic. Lancet Neurol. 2009; 8(5):491–500. S1474-4422(09)70061-4 [pii]. DOI: 10.1016/S1474-4422(09)70061-4 [PubMed: 19375666]
52. Li Y, Chopp M. Marrow stromal cell transplantation in stroke and traumatic brain injury. Neurosci Lett. 2009; 456(3):120–123. DOI: 10.1016/j.neulet.2008.03.096 [PubMed: 19429146]
53. Chopp M, Li Y. Treatment of neural injury with marrow stromal cells. The Lancet Neurology. 2002; 1(2):92–100. [PubMed: 12849513]
54. Chopp M, Li Y, Zhang J. Plasticity and remodeling of brain. J Neurol Sci. 2008; 265(1–2):97–101. DOI: 10.1016/j.jns.2007.06.013 [PubMed: 17610903]
55. Fruhbeis C, Frohlich D, Kuo WP, Amphornrat J, Thilemann S, Saab AS, Kirchhoff F, Mobius W, Goebbels S, Nave KA, Schneider A, Simons M, Klugmann M, Trotter J, Kramer-Albers EM. Neurotransmitter-triggered transfer of exosomes mediates oligodendrocyte-neuron communication. PLoS Biol. 2013; 11(7):e1001604.doi: 10.1371/journal.pbio.1001604 [PubMed: 23874151]
56. Lopez-Verrilli MA, Picou F, Court FA. Schwann cell-derived exosomes enhance axonal regeneration in the peripheral nervous system. Glia. 2013; 61(11):1795–1806. DOI: 10.1002/glia.22558 [PubMed: 24038411]
57. Ha M, Kim VN. Regulation of microRNA biogenesis. Nat Rev Mol Cell Biol. 2014; 15(8):509–524. DOI: 10.1038/nrm3838 [PubMed: 25027649]
58. Winter J, Diederichs S. Argonaute proteins regulate microRNA stability: Increased microRNA abundance by Argonaute proteins is due to microRNA stabilization. RNA biology. 2011; 8(6): 1149–1157. DOI: 10.4161/rna.8.6.17665 [PubMed: 21941127]
59. Aschrafi A, Schwechter AD, Mameza MG, Natera-Naranjo O, Gioio AE, Kaplan BB. MicroRNA-338 regulates local cytochrome c oxidase IV mRNA levels and oxidative

phosphorylation in the axons of sympathetic neurons. J Neurosci. 2008; 28(47):12581–12590. 28/47/12581 [pii]. DOI: 10.1523/JNEUROSCI.3338-08.2008 [PubMed: 19020050]

60. Dajas-Bailador F, Bonev B, Garcez P, Stanley P, Guillemot F, Papalopulu N. microRNA-9 regulates axon extension and branching by targeting Map1b in mouse cortical neurons. Nature Neuroscience. 2012; 15(5):697–699. DOI: 10.1038/nn.3082
61. Lu CS, Zhai B, Mauss A, Landgraf M, Gygi S, Van Vactor D. MicroRNA-8 promotes robust motor axon targeting by coordinate regulation of cell adhesion molecules during synapse development. Philos Trans R Soc Lond B Biol Sci. 2014; 369(1652) 20130517 [pii] rstb.2013.0517 [pii]. doi: 10.1098/rstb.2013.0517
62. Park KK, Liu K, Hu Y, Smith PD, Wang C, Cai B, Xu B, Connolly L, Kramvis I, Sahin M, He Z. Promoting axon regeneration in the adult CNS by modulation of the PTEN/mTOR pathway. Science. 2008; 322(5903):963–966. DOI: 10.1126/science.1161566 [PubMed: 18988856]
63. He Z. Intrinsic control of axon regeneration. Journal of biomedical research. 2010; 24(1):2–5. DOI: 10.1016/S1674-8301(10)60002-4 [PubMed: 23554605]
64. Gardner RT, Habecker BA. Infarct-derived chondroitin sulfate proteoglycans prevent sympathetic reinnervation after cardiac ischemia-reperfusion injury. J Neurosci. 2013; 33(17):7175–7183. DOI: 10.1523/JNEUROSCI.5866-12.2013 [PubMed: 23616527]
65. Xu B, Park D, Ohtake Y, Li H, Hayat U, Liu J, Selzer ME, Longo FM, Li S. Role of CSPG receptor LAR phosphatase in restricting axon regeneration after CNS injury. Neurobiol Dis. 2015; 73:36–48. DOI: 10.1016/j.nbd.2014.08.030 [PubMed: 25220840]
66. Vuppalanchi D, Willis DE, Twiss JL. Regulation of mRNA transport and translation in axons. Results and problems in cell differentiation. 2009; 48:193–224. DOI: 10.1007/400_2009_16 [PubMed: 19582411]
67. Yoo S, van Niekerk EA, Merianda TT, Twiss JL. Dynamics of axonal mRNA transport and implications for peripheral nerve regeneration. Exp Neurol. 2010; 223(1):19–27. DOI: 10.1016/j.expneurol.2009.08.011 [PubMed: 19699200]
68. Willis DE, Twiss JL. Profiling axonal mRNA transport. Methods Mol Biol. 2011; 714:335–352. DOI: 10.1007/978-1-61779-005-8_21 [PubMed: 21431751]
69. Mulcahy LA, Pink RC, Carter DR. Routes and mechanisms of extracellular vesicle uptake. Journal of extracellular vesicles. 2014; :3.doi: 10.3402/jev.v3.24641
70. Corrado C, Raimondo S, Chiesi A, Ciccia F, De Leo G, Alessandro R. Exosomes as intercellular signaling organelles involved in health and disease: basic science and clinical applications. Int J Mol Sci. 2013; 14(3):5338–5366. DOI: 10.3390/ijms14035338 [PubMed: 23466882]
71. Tian T, Zhu YL, Zhou YY, Liang GF, Wang YY, Hu FH, Xiao ZD. Exosome uptake through clathrin-mediated endocytosis and macropinocytosis and mediating miR-21 delivery. J Biol Chem. 2014; 289(32):22258–22267. DOI: 10.1074/jbc.M114.588046 [PubMed: 24951588]
72. Svensson KJ, Christianson HC, Wittrup A, Bourseau-Guilmain E, Lindqvist E, Svensson LM, Morgelin M, Belting M. Exosome uptake depends on ERK1/2-heat shock protein 27 signaling and lipid Raft-mediated endocytosis negatively regulated by caveolin-1. J Biol Chem. 2013; 288(24):17713–17724. DOI: 10.1074/jbc.M112.445403 [PubMed: 23653359]
73. Valapala M, Vishwanatha JK. Lipid raft endocytosis and exosomal transport facilitate extracellular trafficking of annexin A2. J Biol Chem. 2011; 286(35):30911–30925. DOI: 10.1074/jbc.M111.271155 [PubMed: 21737841]
74. Fitzner D, Schnaars M, van Rossum D, Krishnamoorthy G, Dibaj P, Bakhti M, Regen T, Hanisch UK, Simons M. Selective transfer of exosomes from oligodendrocytes to microglia by macropinocytosis. J Cell Sci. 2011; 124(Pt 3):447–458. DOI: 10.1242/jcs.074088 [PubMed: 21242314]
75. Escrevente C, Keller S, Altevogt P, Costa J. Interaction and uptake of exosomes by ovarian cancer cells. BMC Cancer. 2011; 11:108. 1471-2407-11-108 [pii]. doi: 10.1186/1471-2407-11-108 [PubMed: 21439085]
76. Goda Y. SNAREs and regulated vesicle exocytosis. Proc Natl Acad Sci U S A. 1997; 94(3):769–772. [PubMed: 9023331]
77. Xu J, Luo F, Zhang Z, Xue L, Wu XS, Chiang HC, Shin W, Wu LG. SNARE proteins synaptobrevin, SNAP-25, and syntaxin are involved in rapid and slow endocytosis at synapses.

Cell Rep. 2013; 3(5):1414–1421. S2211-1247(13)00117-4 [pii]. DOI: 10.1016/j.celrep.2013.03.010 [PubMed: 23643538]

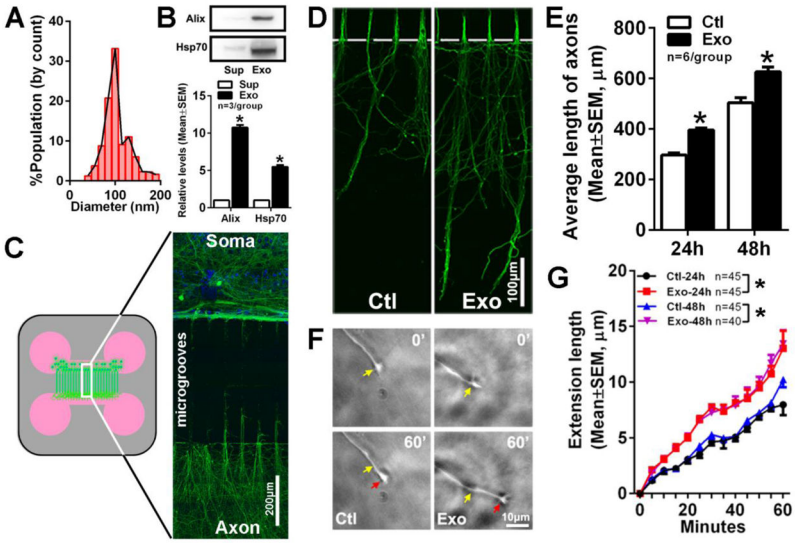

Figure 1. Soma application of MSC-exosomes promotes axonal growth of cortical neurons

A histogram (A) shows particle sizes of MSC-exosomes analyzed by the qNano system. Western blot analysis (B) shows the proteins of Alix and Hsp70 in MSC-exosomes (Exo) and supernatants (Sup). The schematic of a microfluidic culture device and a representative immunofluorescent image (C) show the pNFH+ cortical neurons and axons (green) in the cell body compartment (soma) and pNFH+ axons (green) in the axonal compartment (axon). The compartments are connected by 450 μm long microgrooves (C, microgrooves). DAPI labeled nuclei of cortical neurons (blue) were only present in the cell body compartment (C, soma). Panels D and E show representative images of pNFH+ axons in the axonal compartment (D, green) and quantitative data of the average axonal length (E) from the control (Ctl) and MSC-exosome (Exo) groups when the exosomes were applied into the soma compartment for 24 and 48h. * $p<0.001$ vs control. Panels F and G show representative time-lapse microscopic images of the growth cone extension (F) and quantitative data of growth cone elongation (G) in the axonal compartment during 60 min from the control (Ctl) and MSC-exosome (Exo) groups. Yellow and red arrows in panel F indicate starting (0 min) and ending (60 min) points, respectively. The representative time-lapse microscopic images (F) were acquired from 24h after soma application of the exosomes, whereas quantitative data (G) were acquired for 24 and 48h after exosome application. *$p<0.05$ vs control. Sample size in G represents the number of the growth cone from every independent experiment.

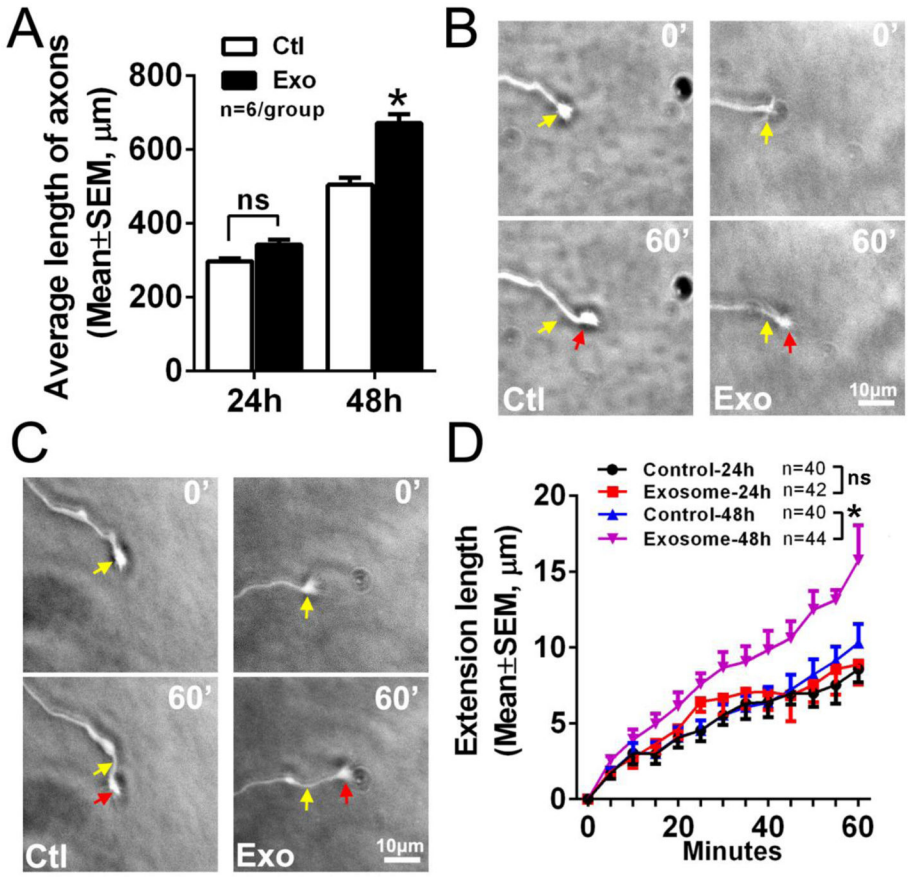

Figure 2. Axonal application of MSC-exosomes locally enhances axonal growth

Quantitative data (A) show the average axonal length in the axonal compartment at 24 and 48h in culture from the control (Ctl) and exosome (Exo) groups, when MSC-exosomes were applied into the axonal compartment. *p<0.001 vs control. Panels B and C are representative time-lapse microscopic images showing elongation of growth cones in the axonal compartment during 60 min from the control (Ctl) and exosome (Exo) groups when experiments were performed 24 (B) and 48h (C) after axonal application of MSC-exosomes. Yellow and red arrows in panels B and C indicate starting (0 min) and ending (60 min) points, respectively. Panel D is quantitative data acquired during a 60 min period. Note, a 24h time point did not show a statistical significance between the control and exosome groups. * p<0.05 vs control. Sample size in D represents the number of the growth cone from every independent experiment.

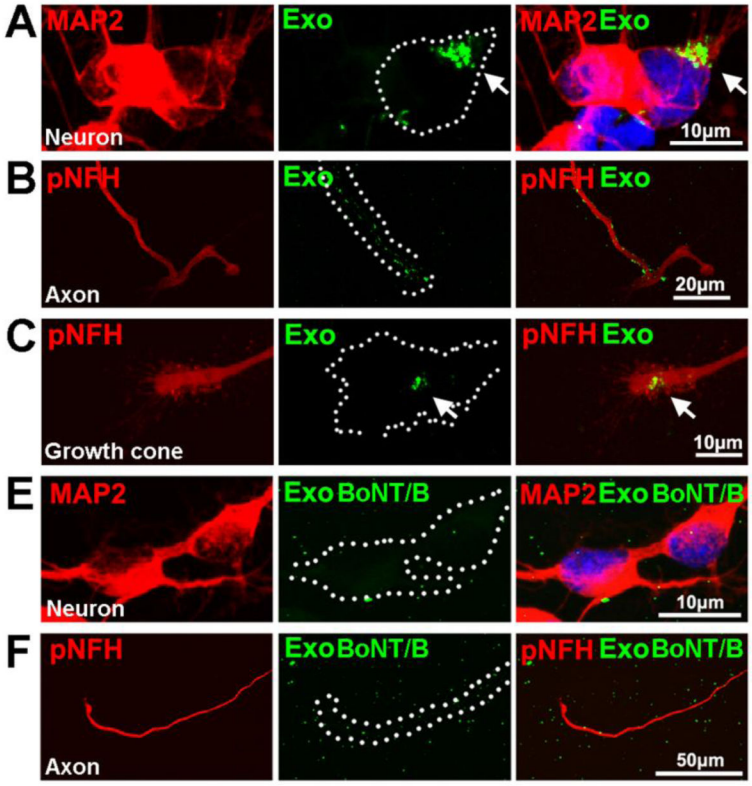

Figure 3. The internalization of MSC-exosomes by cell bodies and distal axons of cortical neurons

Representative confocal immunofluorescent images acquired from the cell body compartment (A, B) show the presence (A) and absence (B) of green fluorescent signals (green) within the cytoplasma of MAP2+ (A, B, red) cortical neurons after soma application of Exo-fect® labeled naive MSC-exosomes (A, Exo) and Exo-fect® labeled exosomes pretreated with BoNT/B (B, Exo BoNT/B), respectively. The nuclei in A and B were labeled with DAPI (blue). Representative immunofluorescent images acquired from the axonal compartment (C, D, and E) show the presence of green fluorescent signals (green) along the pNFH+ distal axon (C, red) and within pNFH+ growth cone (D, red) after axonal application of the Exo-fect® labeled naïve MSC-exosomes (C, D, Exo), whereas green fluorescent signals were randomly distributed apart from the pNFH+ distal axon (E, green) after the axonal application of Exo-fect® labeled MSC-exosomes pretreated with BoNT/B (E, Exo BoNT/B). The white dash line outlines contours of cell bodies, axons, and a growth cone. Each image was a composite image from 5 Z stack images at 0.5μm interval on the growth cone area or 10 Z stack images at 0.5μm interval on the cell body area, respectively.

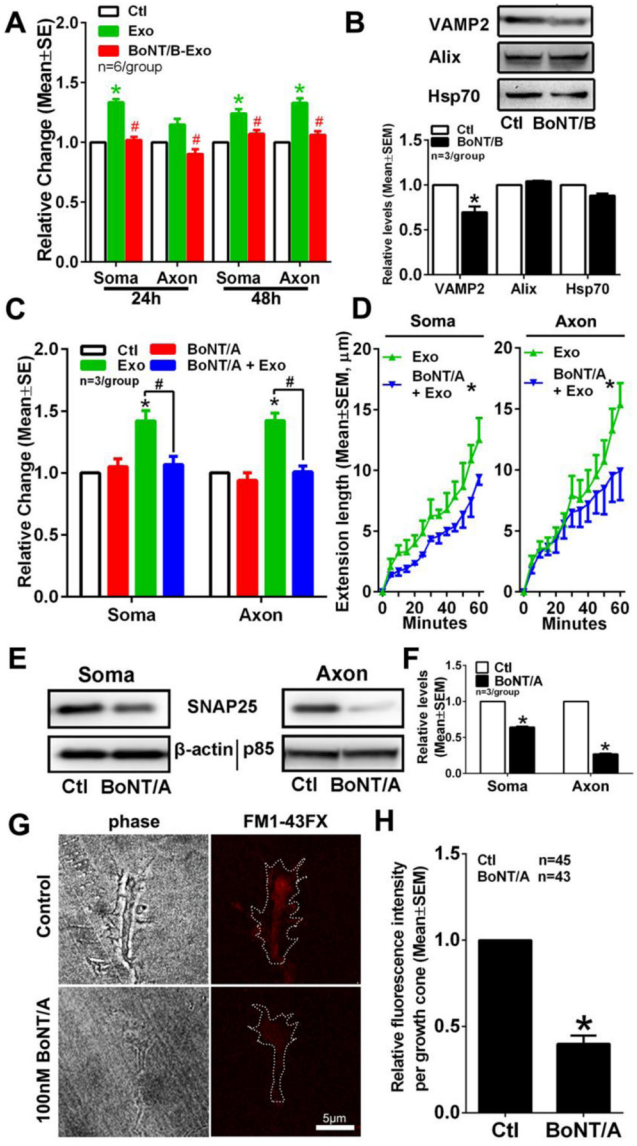

Figure 4. The BoNT/B and BoNT/A treatments abolish the MSC-exosomes increased axonal growth

Quantitative data (A) show the effect of naïve exosomes (exo) and exosomes pretreated with BoNT/B (BoNT/B-Exo) on distal axonal length when the exosomes were applied into the soma (Soma) or the axonal compartment (Axon). Data were normalized to the control group (Ctl). *p<0.05 vs control and #p<0.05 vs naïve exosomes. Representative Western blot images and quantitative data (B) show levels of VAMP2, Alix and Hsp70 proteins in naïve exosomes (Exo) and exosomes pretreated with BoNT/B (BoNT/B). *p<0.05 vs naïve exosomes. Panel C shows the effect of naïve MSC-exosomes on axonal length of the cortical neurons pretreated with BoNT/A (BoNT/A+Exo) for 24h in the cell body (Soma) or the axonal compartment (Axon) compared to the control (Ctl), BoNT/A pretreatment only (BoNT/A) and exosome only (Exo) groups. *p<0.05 vs control and #p<0.05 vs exosome only. Quantitative data of axonal elongation in the axonal compartment (D) show the effect

of the naïve exosomes (Exo) on distal axonal growth of cortical neurons with BoNT/A pretreatment (BoNT/A+Exo) or without BoNT/A pretreatment (Exo) during 60 min of time-lapse microscopic experiments when MSC-exosomes were applied into the somal (Soma, n=45/Exo and 41/BoNT/A+Exo) or axonal (axon, n=44/Exo and 40/BoNT/A+Exo) compartment. *p<0.05 vs exosomes. Representative Western blot images (E) and quantitative data (F) show the effect of BoNT/A treatment on soma and axonal SNAP25 proteins when BoNT/A was applied to the cell body (BoNT/A, Soma) and axonal (BoNT/A, Axon) compartments, respectively, compared to non-treated neurons (Ctl, Soma) and axons (Ctl, Axon). *p<0.05 vs control. Representative microscopic images (G) and quantitative data (H) show the effect of BoNT/A (BoNT/A) treatment on uptake of FM1-43FX dye by axonal growth cones. *p<0.05 vs control (Ctl).

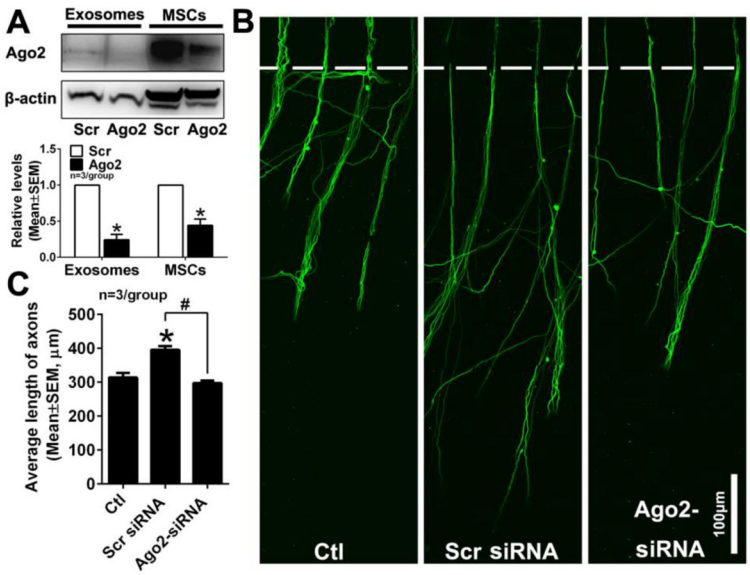

Figure 5. Reduction of Ago2 in MSC-exosomes abolishes exosome-increased axonal growth

Western blot images and quantitative data (A) show levels of Ago2 in MSCs transfected with scramble siRNA (MSCs, Scr) or siRNA against Ago2 (MSCs, Ago2) and Ago2 levels in corresponding exosomes isolated from MSCs (Exosomes). *p<0.05 vs scramble group. Panels B and C show representative immunofluorescent images of pNFH+ axons in the axonal compartment (B) and quantitative data of axonal length (C) in groups of control (Ctl), exosomes from MSCs transfected with scramble siRNA (Scr siRNA) and with siRNA against Ago2 (Ago2-siRNA), when exosomes were applied into the soma compartment of 3 independent experiments. *p<0.05 vs control group and #p<0.05 vs scramble group.

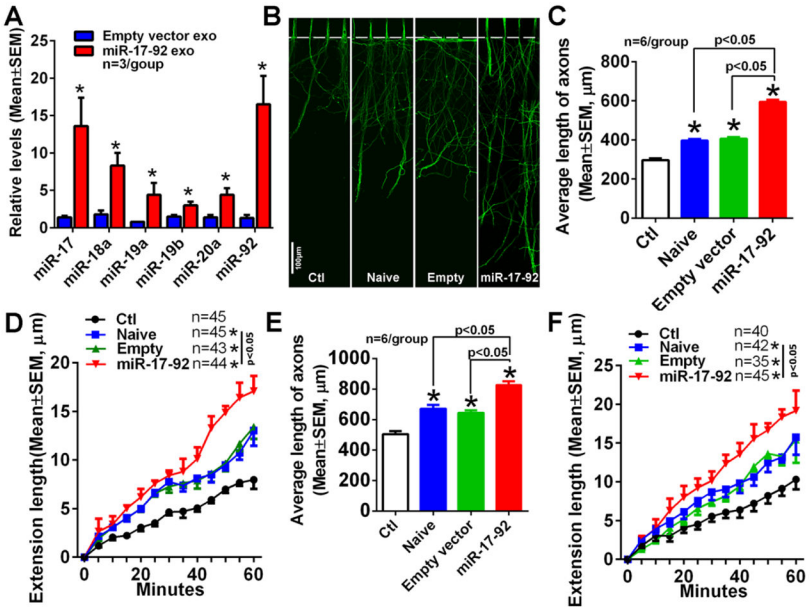

Figure 6. Tailored exosomes with elevated miR-17-92 cluster enhance axonal growth

Quantitative RT-PCR data (A) show relative levels of individual members of miR-17-92 cluster in exosomes derived from MSCs transfected with empty vector (Empty vector exo) and miR-17-92 cluster (miR-17-92 exo). Representative immunofluorescent images of pNFH+ axons in the axonal compartment (B) and quantitative data (C) of average length of axons in groups of control (Ctl) and naïve exosomes (Naïve), empty vector exosomes (Empty), miR-17-92 cluster enriched exosomes (miR-17-92), when exosomes were applied into the soma compartment for 24h. *, $p<0.05$ vs control. Quantitative data of axonal elongation (D) in the axonal compartment from the groups of control (Ctl) and naïve exosomes (Naïve), empty vector exosomes (Empty), miR-17-92 cluster enriched exosomes (miR-17-92) during 60 min of time-lapse microscopic experiments when MSC-exosomes were applied into the soma compartment. * $p<0.05$ vs control group. Panels E and F show quantitative data of average length of axons (E) and axonal elongation during 60 min of time-lapse microscopic experiments (F) from groups of control (Ctl), naïve exosomes (Naïve), empty vector exosomes (Empty), and miR-17-92 cluster enriched exosomes (miR-17-92), when exosomes were applied into the axonal compartment for 48h. * $p<0.05$ vs control group. Sample size in D and F represents the number of the growth cone from every independent experiment.

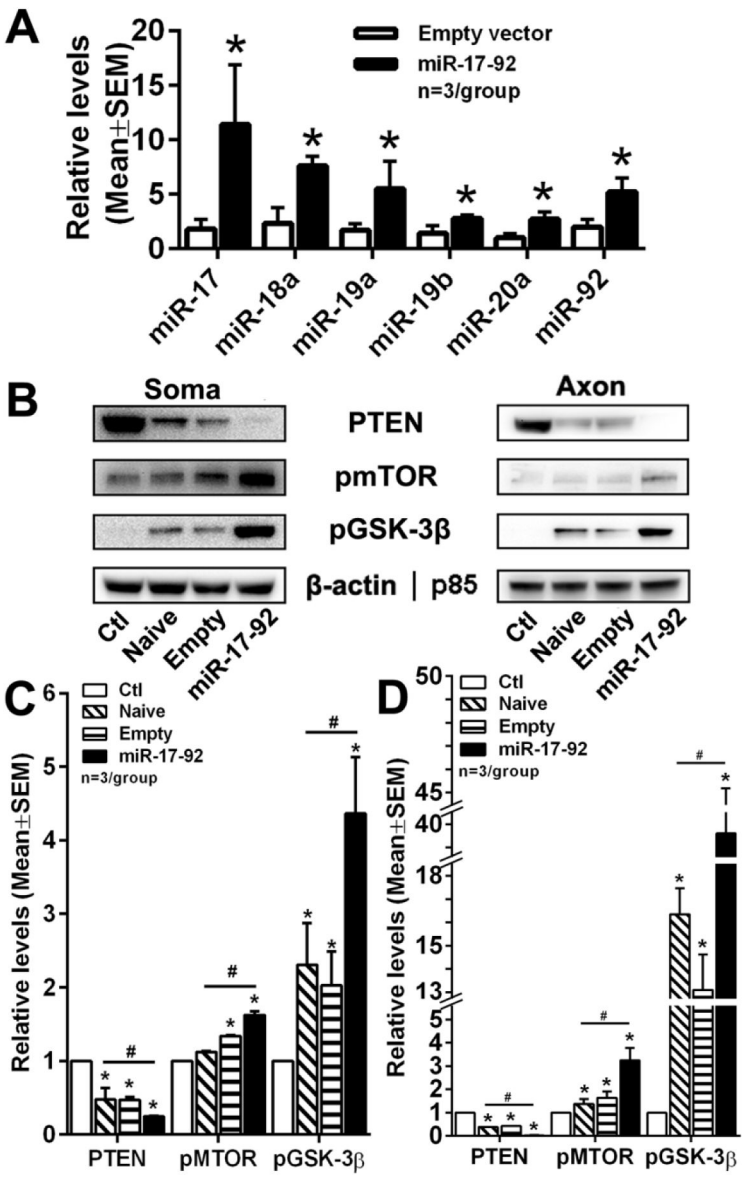

Figure 7. MSC-exosomes modulate the PTEN/mTOR/GSK-3β pathway in soma and distal axons of cortical neurons

Quantitative RT-PCR data (A) show levels of individual members of miR-17-92 cluster within cortical neurons after treatment with empty vector exosomes (Empy vector) or miR-17-92 cluster enriched exosomes (miR-17-92). *p<0.05 vs Empty vector. Representative Western blot images (B) and quantitative data (C, D) show protein levels of PTEN, mTOR, pGSK-3β in somata (C) and distal axons (D) after treatment with naïve exosomes (Naïve), empty vector exosomes (Empty) and miR-17-92 cluster enriched exosomes (miR-17-92), when exosomes were applied into the soma compartment. *p<0.05 vs control group; #p<0.05 vs miR-17-92 group.

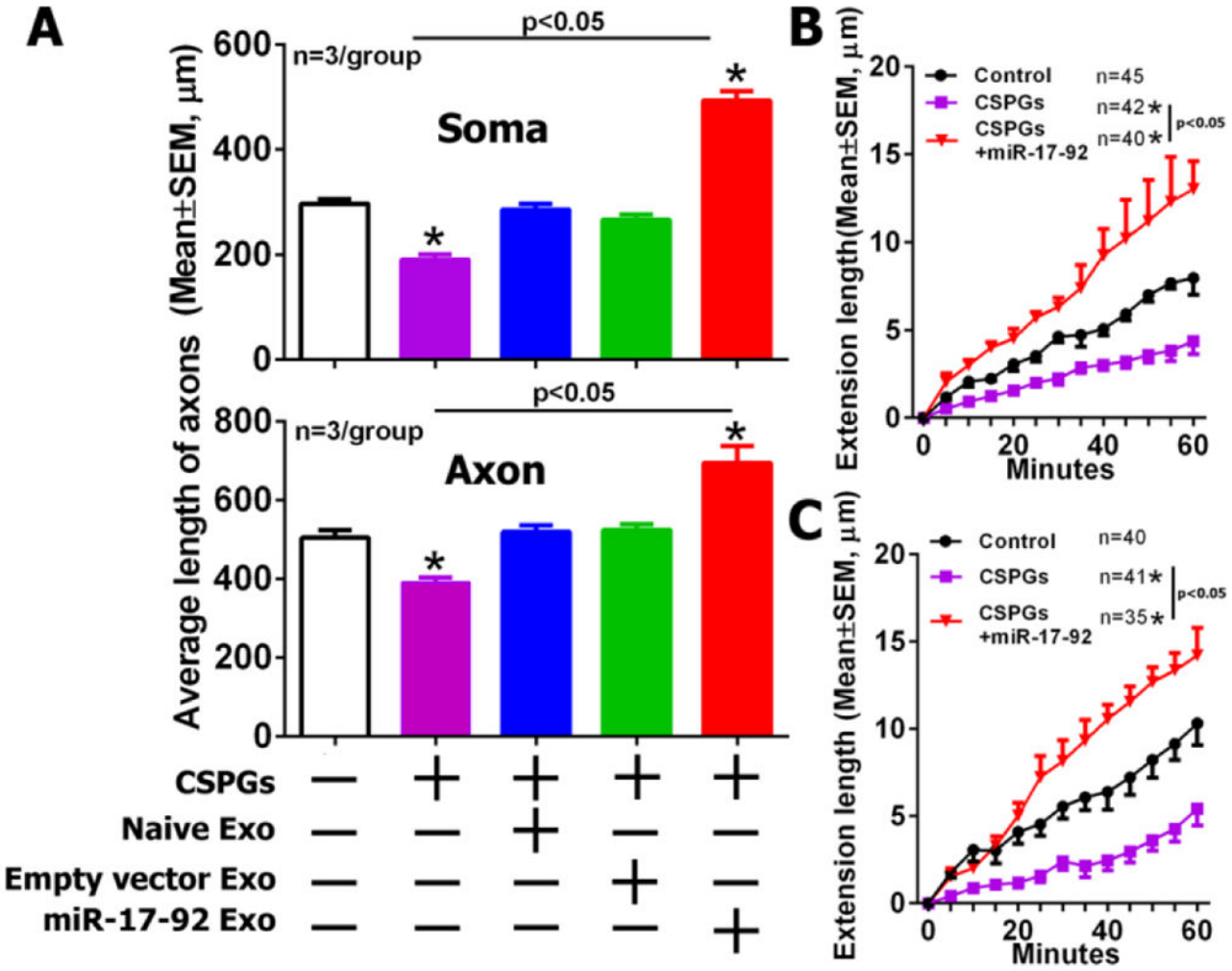

Figure 8. MSC-exosomes overcome the CSPG inhibitory effect on axonal growth

Quantitative data acquired from the axonal compartment (A) show the average length of distal axons in groups of control (white), CSPGs only (Pink), CSPGs with naïve MSC-exosomes (Blue), CSPGs with empty vector MSC-exosomes (Green) and CSPGs with miR-17-92 elevated MSC-exosomes (Red), when CSPGs and exosomes were applied into the cell body (soma, the upper panel) or the axonal compartment (axon, the lower panel). Time-lapse quantitative data acquired from the axonal compartment (B, C) show axonal elongation in groups of control (Control), CSPGs only (CSPGs) and miR-17-92 cluster enriched exosomes under CSPG condition (CSPGs+miR-17-92) during a 60 min of time-lapse microscopic period, when CSPGs and the exosomes were applied into the cell body (B) or axonal compartment (C). *p<0.05 vs control group. Sample size in B and C represents the number of the growth cone from every independent experiment.

Table 1

Top 20 reduced miRNAs within Ago2-decreased MSC-exosomes.

miRNAs	CT values (means±SEM)		p-value
	Scr exosomes (n=3)	Ago2 exosomes (n=3)	
miR-339-3p	27.2±1.2	33.4±1.5	0.032
miR-192	31.3±0.4	34.7±0.5	0.005
miR-423-5p	27.6±0.7	31.0±1.2	0.068
miR-365	25.8±1.0	29.2±1.0	0.072
miR-324-3p	27.5±0.5	30.7±1.8	0.157
miR-132	25.0±0.6	28.2±2.9	0.349
miR-302a	22.9±0.8	26.1±2.6	0.310
miR-410	30.9±2.1	34.0±1.3	0.268
miR-331-3p	28.5±0.4	31.6±1.8	0.165
miR-195	30.2±0.6	33.3±1.2	0.073
miR-320	24.2±0.5	27.1±1.5	0.148
miR-21	25.1±0.7	28.0±2.1	0.256
miR-214	24.4±0.6	27.0±1.7	0.218
miR-106b	28.6±0.3	31.2±1.9	0.238
miR-207	27.5±0.9	30.1±1.6	0.235
miR-125b-5p	24.4±0.8	27.0±1.8	0.259
miR-93	28.8±0.4	31.4±1.8	0.229
miR-125a-3p	28.4±0.3	31.0±0.5	0.015
miR-381	29.7±2.1	32.3±1.4	0.377
miR-30a	26.5±0.9	29.0±1.6	0.252

Data were acquired from Taqman miRNA array analysis. Exosomes derived from MSCs transfected with scramble siRNA (Scr exosomes) and siRNA against Ago2 (Ago2 exosomes).